A GLENCORE COMPANY

Report: Selenium Bioaccumulation Modelling Update for the 2020 – 2022 RAEMP Report

Overview: Bioaccumulation models support the assessment and management of potential effects of selenium on aquatic life by modelling the uptake of less and more bioaccumulative selenium forms into the tissue of aquatic bugs over a range of scenarios.

Being able to model the potential spatial and temporal extent and magnitude of aquatic bug tissue selenium concentrations from organic selenium in surface water allows EVR's Qualified Professionals to estimate the potential risk that selenium in aquatic bug tissue may pose to aquatic bugs and a range of fish species, including the westslope cutthroat trout, in the Elk Valley.

The 2023 model update incorporated data collected between 2020 and 2022 for the total selenium bioaccumulation model for lotic areas, and the speciation model used the 2022 SeSMP dataset for model validation and potential recalibration.

For More Information

If you have questions regarding this report, please:

- Phone: 1-236-484-2200
- Email: **info@evr.glencore.ca**

Future studies will be made available at **Glencore.ca/evr/sustainability/water-quality/water-quality-monitoring**

APPENDIX N
SELENIUM BIOACCUMULATION MODEL

TECHNICAL MEMORANDUM

DATE 30 November 2023 **Reference No.** 023-0001

TO Nick Manklow
Teck Coal Limited

CC Mariah Arnold, Derek Green

FROM Adrian de Bruyn

SELENIUM BIOACCUMULATION MODELLING UPDATE FOR THE 2020-2022 RAEMP REPORT

ADEPT Environmental Sciences Ltd. (ADEPT) is pleased to provide Teck Coal Limited (Teck) with the following update to the selenium bioaccumulation models developed for the Elk Valley.

1.0 BACKGROUND

Bioaccumulation models are used by Teck to help understand how changes to concentrations and/or speciation of selenium in water will affect concentrations in biota, and these models thereby support the assessment and management of potential effects of selenium on aquatic life. Several different model equations have been developed to characterize bioaccumulation under the conditions that occur in different areas of the Elk Valley, and collectively these various equations provide a "toolbox" of options for bioaccumulation modelling.

Teck periodically updates the selenium bioaccumulation models as specified in Permit 107517, issued by BC Ministry of Environment and Climate Change Strategy (ENV) under the provisions of the *Environmental Management Act* on 19 November 2014 and most recently amended 18 May 2023. Section 9.6 states:

> *The RAEMP <Regional Aquatic Effects Monitoring Program> report for the first approved cycle under the ABMP <Area-based Management Plan> must be submitted to the Director by September 30, 2017 and by November 30 of the final year of each subsequent three year monitoring cycle. […] Each report will, on a three year cycle, verify and calibrate the selenium bioaccumulation model using the most recent three years of water quality, aquatic effects and other data from any special studies undertaken.*

As in previous bioaccumulation modelling updates (Golder 2018a, 2020), the focus of the analysis herein is on evaluating and updating model equations that describe the combined uptake of selenium from water into periphyton and trophic transfer from periphyton to benthic invertebrates. The initial uptake step from water into periphyton is the largest step in the selenium bioaccumulation process, typically representing an increment in concentrations from micrograms per litre (µg/L) in water to milligrams per kilogram dry weight (mg/kg dw) in biota. The initial uptake step is also the most variable step, with concentration ratios between biota and water ranging from ~10 to 100,000. The benefit of combining the initial uptake and trophic transfer steps, in addition to avoiding various sources of uncertainty that affect periphyton tissue chemistry, is that the models can incorporate the large dataset of benthic invertebrate tissue selenium data collected by Teck under a wide range of conditions over more than a decade of monitoring.

2.0 HISTORY OF ELK VALLEY BIOACCUMULATION MODELS

Early Models. Selenium bioaccumulation modelling in the Elk Valley began around 2010. Minnow et al. (2011) used regression analysis of data from the 2009 regional monitoring program and previous studies to derive multi-step food-chain models that were subsequently published in Orr et al. (2012). These models showed a clear difference between lentic and lotic areas in the initial uptake of selenium from water to biofilm, but little difference between areas in subsequent trophic transfer steps. At around the same time, Golder (2010) used linear mixed-effects modelling to derive one-step lotic and lentic models to characterize the overall uptake and trophic transfer of selenium from water to invertebrates, fish eggs, and bird eggs. These one-step models were applied in the Environmental Assessment Certificate Application for the Line Creek Operations Phase II Project (Golder 2011).

The EVWQP Model. At the planning stages of the Elk Valley Water Quality Plan (EVWQP; Teck 2014), it was decided in consultation with the Technical Advisory Committee that a new selenium bioaccumulation model would be developed, building on previous efforts and incorporating new data and understanding. The modelling analysis undertaken for the EVWQP evaluated a range of one-step and multi-step approaches to characterize prevailing patterns of selenium bioaccumulation in aquatic habitats of the Elk Valley. A field study was conducted in 2013 to characterize how bioaccumulation varied across many sites in the Elk Valley with a range of lentic habitat characteristics and to delineate the prevalence of areas with lentic-type bioaccumulation (Appendix A to Annex E of the EVWQP). Most of the lentic areas studied, although possessing some degree of lentic characteristics such as fine sediments, slow flow, and aquatic vegetation, had selenium bioaccumulation within the range observed in lotic areas. These areas were provisionally classified as “semi-lentic” and were included in EVWQP model development. The EVWQP model was thus derived to characterize bioaccumulation under the lotic and semi-lentic conditions that were observed to predominate in the Elk Valley. Bioaccumulation in distinct “fully lentic” areas was modelled using the lentic model reported in Orr et al. (2012).

The underlying theory, modelling framework, dataset, statistical derivation, supporting analyses, and evaluation of the EVWQP bioaccumulation model are described in detail in Annex E of the EVWQP (Teck 2014). In brief, the EVWQP model described the uptake of aqueous selenium into periphyton and subsequent trophic transfer to benthic invertebrates, fish, and aquatic-feeding birds. These processes were modelled as a series of regression equations derived from a large dataset of paired selenium concentrations in water and biota measured at dozens of sites throughout the Elk Valley over several decades of studies and monitoring. The final set of model equations selected for the EVWQP was a two-step model. The first step described the combined uptake of aqueous selenium into periphyton and trophic transfer from periphyton to benthic invertebrates in a single model equation, which resulted in improved model performance relative to modelling the processes separately. The second step described trophic transfer of selenium from benthic invertebrate prey to fish or aquatic-feeding birds.

2017 Model Update. The first 3-year model update under Permit 107517 (Golder 2018a) validated the EVWQP (lotic and semi-lentic) and Orr et al. (lentic) models using data collected subsequent to the EVWQP. Golder (2018a) also developed a trophic transfer model for amphibians, evaluated seasonality of bioaccumulation, tested the influence of frequency and timing of aqueous selenium sampling on model performance, validated the fish and bird models with data for species other than those used to derive the models, and tested model performance in Koocanusa Reservoir and Line Creek. Golder (2018a) concluded that the EVWQP model was supported for continued use at lotic and semi-lentic sites, but that the lentic model should be updated and criteria developed to identify which model should be applied at a given site.

Bioaccumulation Tool Version 1. At around the same time as the Golder (2018a) model update, Teck began investigating the effect of selenium speciation on bioaccumulation in Line Creek downstream of the West Line Creek Active Water Treatment Facility (AWTF). Golder (2018b) derived models to predict the bioaccumulation of selenate (from field data) and selenite (from laboratory data), then used these models to infer the bioaccumulation of organic and uncharacterized species, which were at that time collectively referred to as "other" selenium. Separate estimates of the bioaccumulation of "other" selenium were derived for two conditions: i) speciation prior to implementation of an Advanced Oxidation Procedure (AOP) at the AWTF (in which "other" selenium was estimated to be about 10× more bioaccumulative than selenite); and ii) speciation after implementation of AOP (in which "other" selenium was estimated to be about as bioaccumulative as selenite). The resulting speciation bioaccumulation model was referred to at that time as the "bioaccumulation tool" and subsequently as the "b-tool".

2020 Model Update. The second 3-year model update (Golder 2020) implemented the recommendations of Golder (2018a) by recalculating the EVWQP and Orr et al. (2012) models using an updated dataset of paired aqueous total selenium and benthic invertebrate tissue selenium concentrations. Building on learnings from the speciation studies described above, the EVWQP model update focused on characterizing bioaccumulation at lotic sites with speciation typical of most mine-affected waters in the Elk Valley. Sites downstream of the West Line Creek AWTF and immediately downstream of some sedimentation ponds were identified as having atypical speciation that caused a flaring out of residual variance at high aqueous selenium concentrations and poor fit to data from the majority of sites. To avoid conflating these different patterns of bioaccumulation in different areas, it was recommended that these atypical sites be excluded from the lotic total selenium model and instead modelled using the Golder (2018b) speciation model. The resulting updated lotic model was derived from a larger dataset (571 versus 291 paired observations) and had improved performance relative to the EVWQP model. Golder (2020) also updated the lentic model, increasing the underlying dataset from 14 to 174 paired observations. The updated lentic model focused on characterizing bioaccumulation at "fully lentic" sites and evaluated site characteristics that could be used to predict the occurrence of such conditions.

Bioaccumulation Tool Version 2. Following the initiation of speciation monitoring in 2017, Teck generated a large dataset of paired aqueous speciation and benthic invertebrate tissue selenium concentrations. This dataset was used by de Bruyn and Luoma (2021) to update the speciation model. The model structure was updated to separate "other" selenium into the three organoselenium species that had been detected with sufficient frequency to support analysis: dimethylselenoxide (DMSeO), methylseleninic acid (MeSe(IV)), and methaneselenonic acid (MeSe(VI)). Model equations were updated for selenate (with additional field data) and selenite (with additional laboratory data). These equations were then used to fit model terms describing the bioaccumulation of DMSeO, MeSe(IV), and MeSe(VI) at sites with detectable organoselenium, corresponding to the "atypical" sites that were excluded from the Golder (2020) lotic model update. The resulting updated model exhibited good performance in explaining patterns of bioaccumulation at sites both with and without detectable organoselenium.

de Bruyn and Luoma (2021) recommended that lotic areas without significant influence of organoselenium could be modelled using either the inorganic (selenate and selenite) equations of the updated speciation model or the Golder (2020) total selenium lotic model. The latter has the advantages of not requiring speciation information, which makes it easier to apply in a predictive analysis, and also was derived from a larger dataset than could be considered in development of the speciation model. Results from the two modelling approaches were comparable across areas of the Elk Valley with no detectable organoselenium.

3.0 2023 BIOACCUMULATION MODEL UPDATES

As noted by de Bruyn and Luoma (2021), the total selenium bioaccumulation models (most recently updated in Golder 2020) and speciation models (most recently updated in de Bruyn and Luoma 2021) are equally valid ways of modelling selenium bioaccumulation, and each has its own strengths and limitations. Therefore, this 2023 model update will update both approaches and will lay out how the two approaches can be used as alternatives or in combination, depending on the intended application. The various total selenium and speciation model equations are components of a bioaccumulation modelling toolbox that has greater flexibility than either type of model alone and can capitalize on strengths of each approach while mitigating limitations.

To meet requirements under Section 9.6 of Permit 107517, the following section presents analyses to verify and, where warranted, recalibrate the selenium bioaccumulation model equations based on total selenium (Section 3.1) and speciation (Section 3.2). Section 4 provides recommendations for how these model equations can be used as alternatives or in combination, depending on the intended application.

3.1 Total Selenium Model Updates

Monitoring throughout the Elk Valley since the last 3-year update has generated a large new dataset to validate the Golder (2020) total selenium model for lotic areas, whereas relatively few new data are available for lentic areas. Therefore, the analysis that follows focuses on validation and potential updates to the lotic total selenium model. Validation and potential updates to the lentic total selenium model will be undertaken in the next 3-year update in 2027, when it is anticipated that sufficient new data will be available to support an informative analysis.

Data Preparation

Data for validation and potential recalibration of the lotic total selenium model were obtained from Teck's EQuIS database. All lotic sampling events with benthic invertebrate tissue selenium and concurrent aqueous total selenium data were compiled, replicate results were averaged, and data were screened as in Golder (2020) to exclude locations with an observed or suspected "atypical" pattern of bioaccumulation, which is now understood to relate to the localized influence of organoselenium in certain areas (Table 1). After screening, the compilation included 374 new sampling events between 2020 and 2022.

Table 1. Monitoring areas with observed or suspected atypical selenium speciation

Area Type	Monitoring Areas
Tributaries downstream of mine ponds	RG_BOCK, RG_CLODE, RG_GATE, RG_GHCKD, RG_GHBP, GH_WADE2, EV_HASP_DS2, LC_LC7SP_DS, FR_SCCBO, RG_HACKDS, EV_HASP_DS1, EV_HASP_US, EV_DCSP_DS1, GH_GH1A, GH_GH1SP_DS1, RG_GATEDP, FR_EC1A, GH_UTSP_DS1, RG_LILC3, LC_LC3, LC_DC1, LC_DC4, LC_DCDS, LC_DC2, RG_ERCKDT[a]
Other areas with detectable organoselenium	RG_FODGH, GH_GH1SP_DS3, RG_FOBCP, EV_DCSP_US, GH_UTSP_US, RG_WED, RG_GHNF

[a] RG_ERCKDT has detectable organoselenium and also exhibits enhanced bioaccumulation that is currently understood to relate to particles released from the Elkview Saturated Rock Fill and trapped in dense bryophyte beds immediately downstream of the outfall in Erickson Creek

Validation of the Total Selenium Model

New data (*n*=374 from 2020–2022) are plotted on Figure 1 in comparison to the Golder (2020) lotic dataset (*n*=565 from 1996–2019) and the lotic total selenium model that was derived from that dataset. Figure 2 shows model residuals for the new data in comparison to the Golder (2020) lotic dataset.

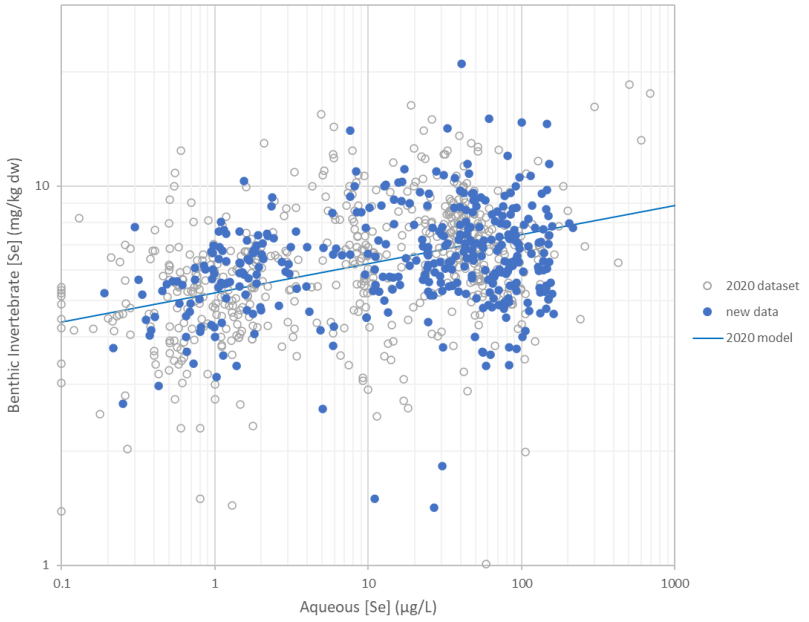

Figure 1. New data (2020-2022) overplotted on the Golder (2020) dataset (1996-2019) and lotic model

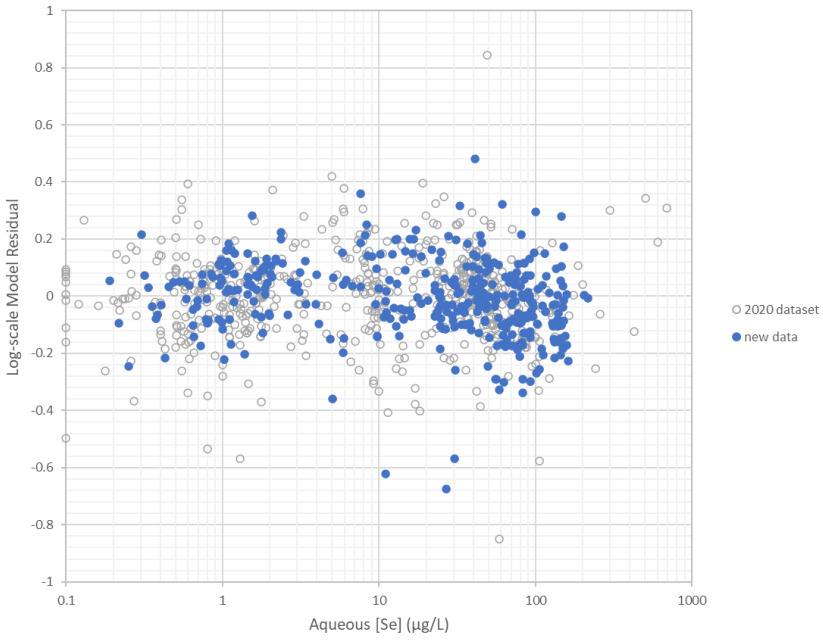

Figure 2. Model residuals for new data (2020-2022) overplotted on residuals of the Golder (2020) dataset

Figures 1 and 2 both show good conformance of new data to the general pattern and degree of scatter evident in the Golder (2020) dataset. Residuals were evenly distributed and exhibited only slight curvature, consistent with patterns described by Golder (2020). New data were within a factor of 1.5 of model predictions for 85% of observations (compared to 80% for the Golder 2020 dataset) and within a factor of 2 of model predictions for 97% of observations (compared to 94% for the Golder 2020 dataset). In short, new data exhibited less residual scatter around the Golder (2020) lotic model than the dataset used to derive that model. Based on this good conformance, recalibration of the lotic total selenium model is not warranted at this time.

3.2 Speciation Model Updates

ADEPT et al. (2023) conducted an evaluation of the de Bruyn and Luoma (2021) speciation model using data collected in the 2022 Selenium Speciation Monitoring Program (SeSMP). This evaluation indicated that the pattern of bioaccumulation evident in the 2022 SeSMP dataset broadly overlapped with the pattern evident in previous data used to derive the speciation model, indicating that the model provided a reasonable characterization of these patterns. However, the speciation model performed slightly less well overall for the 2022 dataset compared to the dataset used to derive the model. It was recommended that the de Bruyn and Luoma (2021) speciation model should be re-evaluated relative to all available data collected since its derivation and, if warranted, recalibrated using an updated dataset. The following section presents those analyses.

Data Preparation

Data for validation and potential recalibration of the speciation model were obtained from Teck's EQuIS database. All lotic sampling events with benthic invertebrate tissue selenium and concurrent aqueous selenium speciation data were compiled and replicate results were averaged. The compilation was then screened to identify sampling events with increased potential for decoupling of tissue selenium concentrations from the concurrent speciation data. The intention was that the following analysis would characterize how aqueous speciation affects bioaccumulation, and for this purpose it was necessary that all sampling events included in the analysis have aqueous speciation measurements that reasonably represent the speciation conditions that caused the observed benthic invertebrate tissue selenium concentrations. Rationale for excluding certain data from the following analysis is provided in Table 2.

After removing cases for the reasons outlined in Table 2, the compilation contained 580 sampling events, including 319 sampling events with no detectable organoselenium (0.148–252 µg/L selenate; <0.01–0.706 µg/L selenite) and 261 sampling events with detectable organoselenium (0.047–371 µg/L selenate; 0.069–6.33 µg/L selenite; <0.01–0.434 µg/L DMSeO; <0.01–0.676 µg/L MeSe(IV)). MeSe(VI) was analyzed in 522 samples and detected in 21 of these (<0.01–0.053 µg/L), 20 of which were in Line Creek downstream of the West Line Creek AWTF. The volatile species DMDSe and DMSe were analyzed in 124 samples and one or both was detected in 22 of these (<0.022-0.144 µg/L DMDSe; <0.022-0.446 µg/L DMSe), all of which were collected immediately downstream of sedimentation ponds and also contained detectable DMSeO and/or MeSe(IV). The single detection of MeSe(VI) outside of Line Creek and the highest concentrations of DMDSe and DMSe in the dataset all occurred in the same sample, which was collected 15 August 2022 immediately downstream of Milligan Creek Sedimentation Pond.

Table 2. Sampling events with increased potential for decoupling of tissue from aqueous speciation

Excluded sampling events	Rationale
All data collected November – February (*n*=202)	Lower vital rates in winter months cause tissue selenium concentrations to change relatively slowly, whereas aqueous organoselenium and selenite concentrations in lotic areas typically decline rapidly in late fall due to flushing of sedimentation ponds. Therefore, lotic biota can continue to reflect speciation in prior months that is not represented by concurrent speciation data. This temporal decoupling means that tissue selenium concentrations in winter may not be directly attributable to aqueous speciation in winter.
Data collected in Erickson Creek immediately downstream of the Elkview Saturated Rock Fill (SRF) outfall (*n*=9)	Erickson Creek immediately downstream of the Elkview SRF outfall exhibits enhanced bioaccumulation that is currently understood to relate to particles released from the SRF and trapped in dense bryophyte beds. This exposure pathway causes bioaccumulation that is not directly related to aqueous speciation measured in overlying water.
Data collected after mitigation causing a step-change reduction in aqueous organoselenium concentrations (*n*=3 in Line Creek; *n*=25 in LCO Dry Creek)	Monitoring following implementation of AOP at the West Line Creek AWTF showed a gradual decline in downstream tissue selenium concentrations through 2018, despite an immediate decline in aqueous organoselenium concentrations. A similar temporal decoupling was observed through 2020 following bypass of the sedimentation ponds at LCO Dry Creek. In both cases, there was an extended period during which bioaccumulation continued to reflect prior high organoselenium concentrations and could not be attributed to concurrent aqueous speciation.
Data collected immediately downstream of sedimentation ponds after apparent flushing events (*n*=7)	ADEPT (2022) concluded that high rainfall events in summer can cause a sudden "reset" of accumulated speciation in a sedimentation pond, resulting in a short-term condition of low aqueous organoselenium concentrations immediately downstream. The drop in organoselenium concentrations and subsequent return to pre-flushing levels occurs more rapidly than biota selenium concentrations can change in response, resulting in a temporary decoupling. This decoupling was identified at locations where organoselenium concentrations were notably lower (usually zero) compared to sampling events in previous and/or subsequent weeks.

Validation of the Speciation Model

Validation was conducted by applying the speciation model to the full updated dataset and evaluating model performance compared to the dataset originally used to derive the model. Performance of the speciation model on the original (de Bruyn and Luoma 2021; open grey symbols) and updated (this study; open and filled blue symbols) datasets is illustrated on Figures 3 and 4. Figure 3 shows measured benthic invertebrate selenium concentrations relative to model predictions. Good model performance would be apparent on this plot as an even distribution of measured values above and below the 1:1 line (solid diagonal), with an approximately equal degree of residual scatter across the modelled range and the majority of observations falling within a factor of 2 of model predictions (dashed diagonals).[1] Figure 4 shows the residual scatter plotted relative to organoselenium concentrations. Good model performance would be apparent on this plot as an even distribution of log-scale residuals above and below zero (solid horizontal line), the absence of slope, curvature, or other structure, approximately equal spread of residuals in all parts of the modelled range, and the majority of values within $\pm\log_{10}(2)$ of zero (dashed horizontal lines).

[1] Although lower residual scatter around the 1:1 line indicates better model performance, residual scatter arises from irreducible spatial and temporal heterogeneity, sampling and analytical variability, and factors affecting bioaccumulation that are unrelated to speciation, and can never be zero.

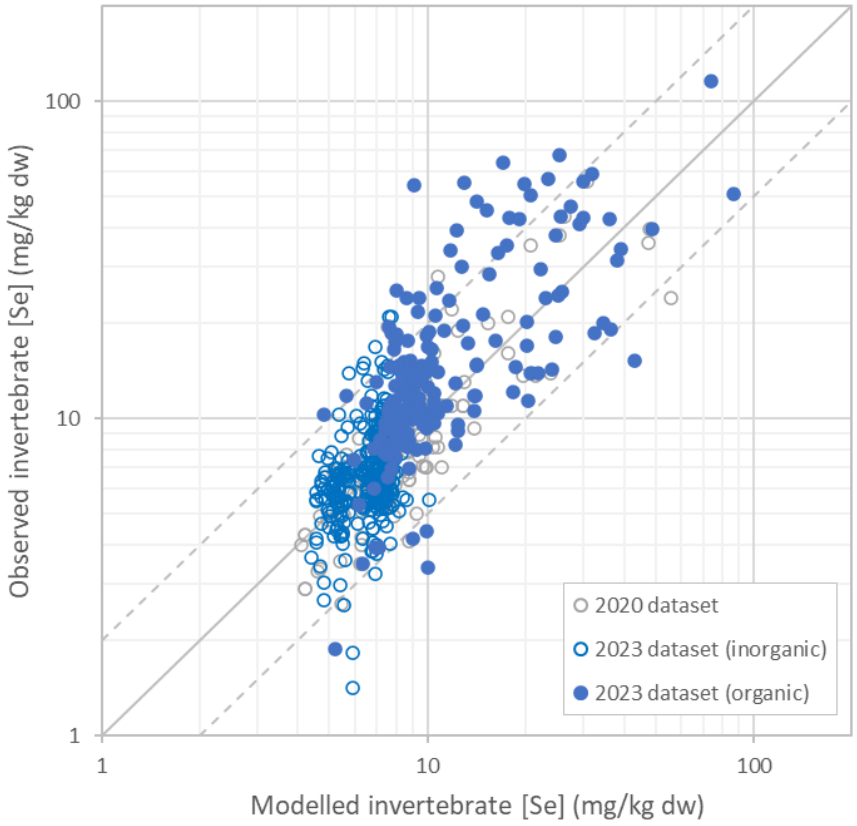

Figure 3. Performance of the de Bruyn and Luoma (2021) model on the updated 2023 dataset

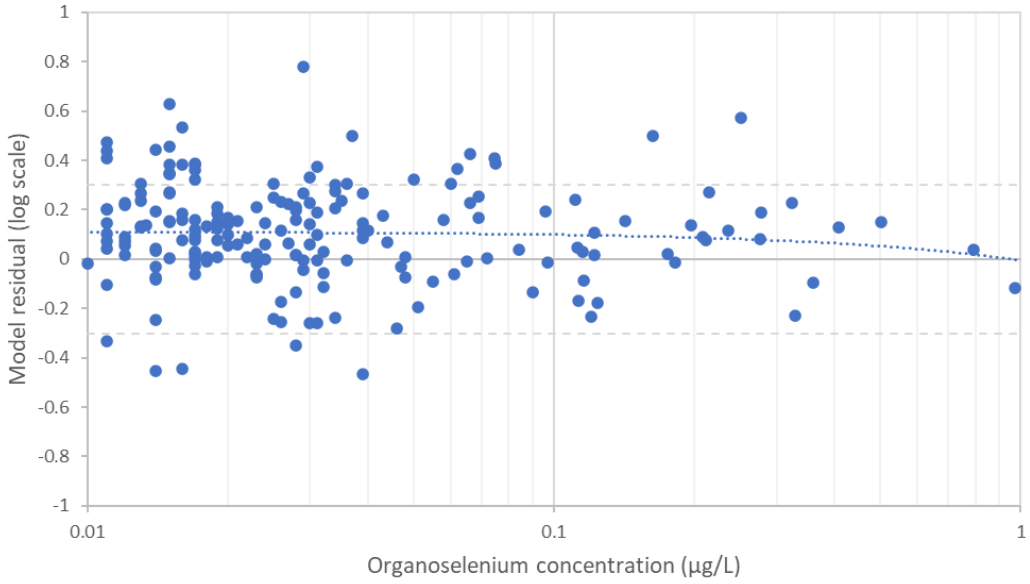

Figure 4. Residuals of the de Bruyn and Luoma (2021) model applied to the updated 2023 dataset

The pattern of measured vs. modelled concentrations on Figure 3 shows inconsistent performance of the speciation model when applied to the updated dataset. Most samples in the updated dataset with no detectable organoselenium (open blue symbols) fell within a factor of 2 of the 1:1 line. However, in samples with detectable organoselenium (filled blue symbols), more were above vs. below the 1:1 line, especially below a modelled benthic invertebrate selenium concentration of 10 mg/kg dw. About one-third of samples with a modelled benthic invertebrate selenium concentration >10 mg/kg dw had measured concentrations more than a factor of 2 higher than the model prediction (Figure 3). These patterns are also apparent on Figure 4: most residuals were positive and often greater than $\log_{10}(2)$ at the low end of organoselenium concentrations. Overall, the speciation model did not perform as well on the updated dataset as on the original dataset, indicating that recalibration was warranted.

Recalibration of the Speciation Model: Overview

Recalibration of the speciation model followed the same general approach used in previous versions because the updated dataset presents similar opportunities and challenges to datasets used to derive previous versions. The main opportunity is the potential to infer the contribution of each species to bioaccumulation in nature by fitting model coefficients to the large available field dataset, which covers a wide range of concentrations of all four frequently-detected species (selenate, selenite, MeSe(IV), and DMSeO). The main challenge is strong multicollinearity among inorganic and organic selenium species concentrations, as noted by de Bruyn and Luoma (2021) in the dataset compiled for their analysis.

Multicollinearity in the speciation dataset likely occurs because selenite and organoselenium are generated via related biological processes (producing collinearity among reduced species) that are enhanced in sedimentation ponds, which is also where concentrations of selenate tend to be highest (producing collinearity between selenate and reduced species). Multicollinearity is apparent in the updated dataset, both between inorganic species across the entire measured range (Figure 5A) and between the two organic species that are frequently detected immediately downstream of sedimentation ponds (Figure 5B). Organoselenium was detected in about two-thirds of samples at >20 µg/L selenate but only about one-tenth of samples at <20 µg/L selenate (Figure 6A), reflecting the influence of sampling locations immediately downstream of sedimentation ponds. The outcome of these underlying multicollinear patterns is a “flaring out” of benthic invertebrate tissue selenium concentrations at the high end of measured aqueous total selenium concentrations (Figure 6B) that coincides with relatively high concentrations of all four frequently-detected species. The lower portion of the data cloud on Figure 6B conforms to the pattern on Figure 1, reflecting the bioaccumulation of selenate and selenite.

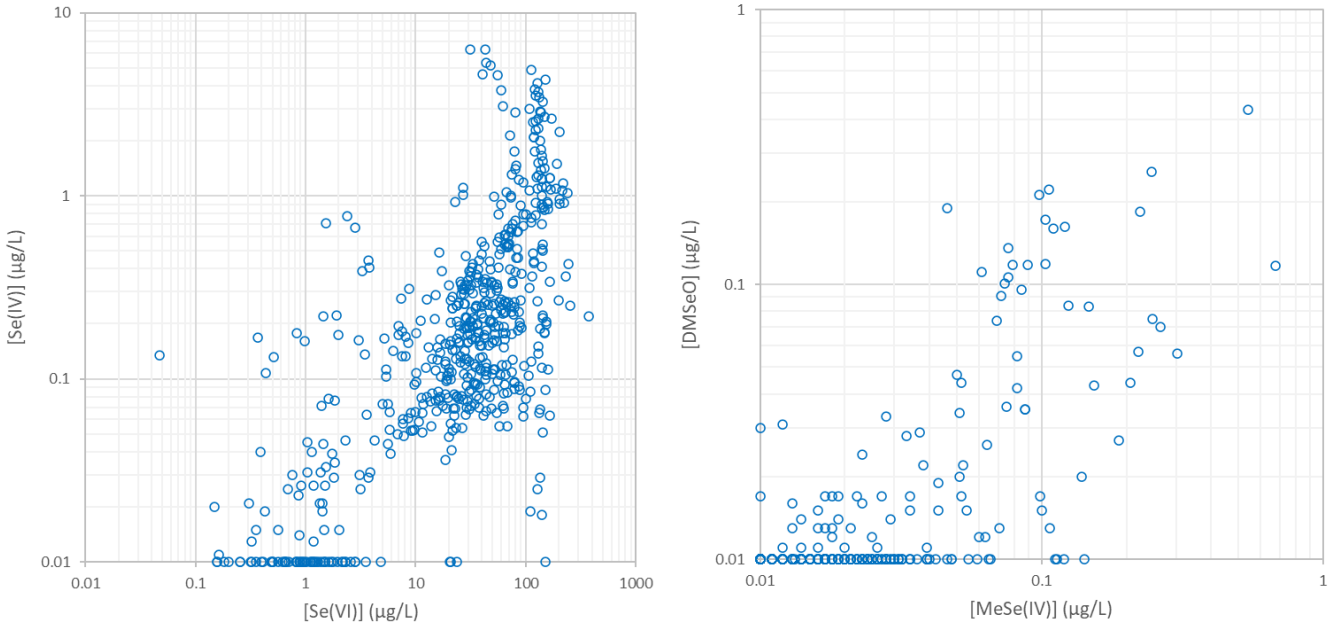

Figure 5. Collinearity between inorganic (left) and organic (right) selenium species in the updated dataset

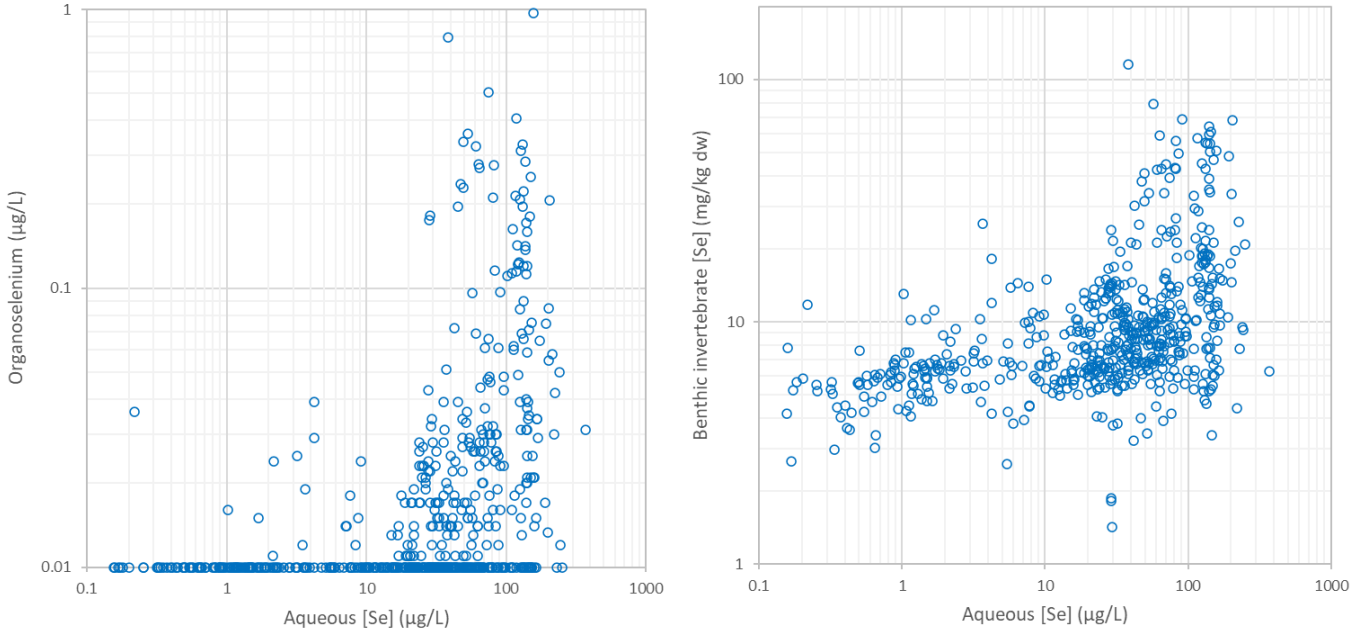

Figure 6. Collinearity of organoselenium (left) and benthic invertebrate selenium (right) with total aqueous selenium

Multicollinearity can be a major issue for regression analysis because it prevents the estimation of robust model coefficients. The usual approach to overcoming multicollinearity is to remove collinear variables or reduce them to orthogonal factors via approaches such as partial least squares regression. However, if there is a mechanistic basis for inclusion of predictor variables, as there is for the present analysis, then removing variables leads to an incomplete model and a mechanistically inaccurate characterization of the effect of retained variables. In this case, a better approach to overcoming multicollinearity is to increase orthogonality between variables, either by conducting more experiments (usually not possible when relying on observational data) or by selecting subsets of the data in which there is less collinearity among variables. de Bruyn and Luoma (2021) took the latter approach, first fitting model coefficients for inorganic species using a subset of data with no detectable organoselenium, then applying these fitted coefficients to fit model coefficients for organic species using a separate subset of data. Strong collinearity between inorganic species prevented the estimation of a robust concentration-dependence slope for selenite, which de Bruyn and Luoma (2021) overcame by adopting a slope from laboratory studies.

The analysis herein adopted the same approach to addressing multicollinearity as de Bruyn and Luoma (2021). To avoid conflating bioaccumulation of inorganic and organic species, the recalibration was conducted in two parts. In part one, a subset of data was identified that reflected only the bioaccumulation of selenate and selenite, and model coefficients for selenate and selenite were fit using that subset. In part two, these inorganic species model coefficients were applied to an expanded model form that included terms for organic species, and model coefficients for organic species were fit using a subset of data that contained detectable organoselenium. In both parts, additional steps were taken to further reduce collinearity and evaluate robustness of model coefficients.

Recalibration of the Speciation Model: Inorganic Species

Recalibration of the selenate and selenite coefficients was conducted as follows:

- The analysis was conducted using the updated dataset described in the **Data Preparation** subsection above, filtered to retain only cases with no detectable organoselenium (*n*=319)
- The same model form used in de Bruyn and Luoma (2021) was adopted, rearranged to give Equation 1
- The nonlinear regression function of Systat v13 was used to fit the coefficients in Equation 1 for selenate (a_{SeVI}, b_{SeVI}, and b_{SO4}) and selenite (a_{SeIV} and b_{SeIV})
- The nonlinear regression analysis was repeated with b_{SeIV} fixed to the value of -0.3 estimated by de Bruyn and Luoma (2021) from controlled laboratory studies
- To reduce effects of collinearity between selenate and selenite, the two nonlinear regression analyses (fitted vs. fixed b_{SeIV}) were repeated using a constrained inorganic dataset that only included cases with selenite concentrations >0.05 µg/L (*n*=215)
- Candidate fitted models were evaluated by inspecting regression statistics and model residuals when applied to the full inorganic dataset of all cases with no detectable organoselenium

The fitted model form was:

$$log_{10}([Se]_{BI}) = log_{10}([SeVI] \times a_{SeVI} \times [SeVI]^{b_{SeVI}} \times [SO_4]^{b_{SO4}} + [SeIV] \times a_{SeIV} \times [SeIV]^{b_{SeIV}}) \quad \text{Equation 1}$$

where $[Se]_{BI}$ is benthic invertebrate selenium concentration (mg/kg dw), [SeVI] is selenate concentration (µg/L), [SeIV] is selenite concentration (µg/L), and $[SO_4]$ is sulphate concentration (mg/L). The coefficients denoted a are intercepts and the coefficients denoted b are concentration-dependence slopes. The model was fit in log space to stabilize residual variance and linearize relationships.

Figure 7 shows the degree of collinearity between selenate and selenite in the inorganic dataset used for this analysis (filled blue symbols) and in the organic dataset not used for this analysis (open grey symbols). Filled blue symbols in the dashed box on Figure 7 are the constrained subset of data (SeIV >0.05 µg/L) used in supplemental analysis to reduce collinearity. Fitted coefficients and regression statistics are provided in Table 3. Model fit and residuals are shown in Figure 8 (full inorganic dataset) and Figure 9 (SeIV >0.05 µg/L).

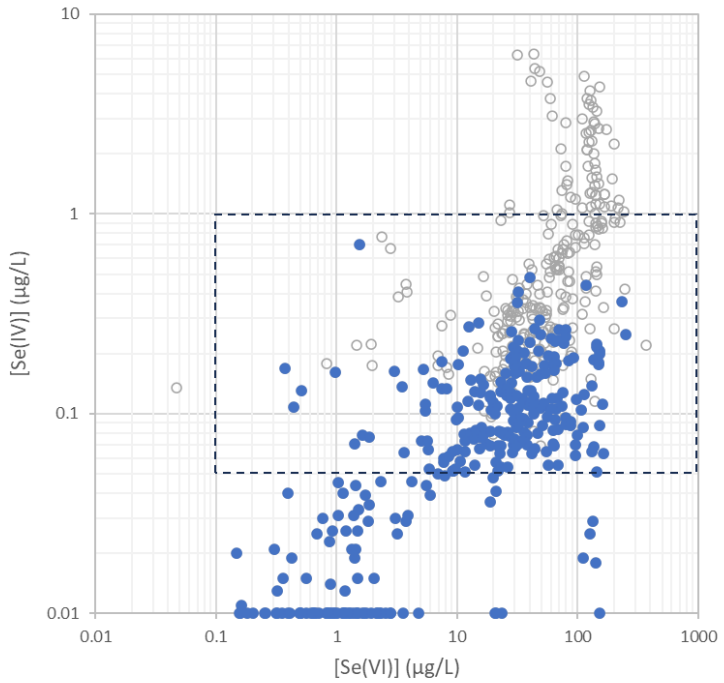

Figure 7. Selenate and selenite concentrations in samples with no detectable organoselenium (filled blue symbols, used to recalibrate inorganic species terms), the constrained dataset with [Se(IV)]>0.05 µg/L (filled blue symbols within the dashed box, used in supplemental analysis), and samples with detectable organoselenium (open grey symbols, not used to recalibrate inorganic species terms)

Table 3. Candidate model coefficients for inorganic species

Parameter	Candidate 1	Candidate 2	Candidate 3	Candidate 4
Approach for selenite	fitted b_{SeIV}	fixed b_{SeIV}	fitted b_{SeIV}	fixed b_{SeIV}
Data included	All; n=319	All; n=319	[SeIV] >0.05; n=215	[SeIV] >0.05; n=215
Mean Corrected r^2	0.157	0.156	0.074	0.072
a_{SeVI}	7.36 (5.74; 8.97)	7.30 (5.69; 8.91)	7.01 (2.86; 16.9)	7.94 (5.16; 10.7)
b_{SeVI}	-0.902 (-0.944; -0.86)	-0.903 (-0.946; -0.861)	-0.858 (-1.23; -0.485)	-0.881 (-0.957; -0.805)
b_{SO4}	-0.083 (-0.147; -0.019)	-0.083 (-0.147; -0.018)	-0.148 (-0.552; 0.257)	-0.126 (-0.225; -0.026)
a_{SeIV}	3.43 (-1.96; 8.82)	2.47 (-0.021; 4.96)	4.22 (-2.89; 11.3)	4.13 (0.286; 7.97)
b_{SeIV}	-0.064 (-1.30; 1.18)	-0.3	-0.622 (-2.76; 1.51)	-0.3

Notes: See text for definitions of parameter names; values in parentheses are 95% confidence intervals on parameter estimates.

All four sets of candidate model coefficients provided similarly reasonable fit to the inorganic dataset and all but candidate 3 had acceptable residuals. All four gave similar estimates of the enrichment factor (K_d) of selenate (~2,000 at 1 µg/L; ~200 at 10 µg/L; ~20 at 100 µg/L), differing mainly in their estimates for selenite.

The candidate model coefficient sets in which b_{SeIV} was fitted were not able to robustly estimate this parameter. Fitting b_{SeIV} to the full inorganic dataset (candidate 1) gave an estimate of -0.064 with a confidence interval that included zero (-1.30; 1.18). Fitting b_{SeIV} to the constrained dataset (candidate 3) gave an estimate of -0.622, but with a wider confidence interval that also included zero (-2.76; 1.51). Candidate 3 also tended to underestimate bioaccumulation at [Se(IV)] <0.05 µg/L, resulting in structured residuals at these concentrations (Figure 9, upper panel). Neither of these estimates is consistent with the results of controlled laboratory experiments summarized in de Bruyn and Luoma (2021) that showed a concentration dependence slope consistently near -0.3.

The candidate model coefficient sets in which b_{SeIV} was fixed at the laboratory-derived estimate of -0.3 differed primarily in the parameter a_{SeIV}, indicating the magnitude of selenite bioaccumulation estimated by the model. The candidate model coefficients fit to the full inorganic dataset (candidate 2) had a fitted a_{SeIV} of 2.47, which gives estimates of K_d for selenite ranging from 1,762 at 0.1 µg/L to 883 at 1 µg/L. The candidate model coefficients fit to the constrained inorganic dataset (candidate 4) had a fitted a_{SeIV} of 4.13, which gives estimates of K_d for selenite ranging from 2,942 at 0.1 µg/L to 1,474 at 1 µg/L. Candidate 4 was more consistent with the estimates of 720 to 2,800 derived by Presser and Luoma (2010) and fell in the middle of results from laboratory studies of selenite uptake (Figure 10), and was therefore selected.

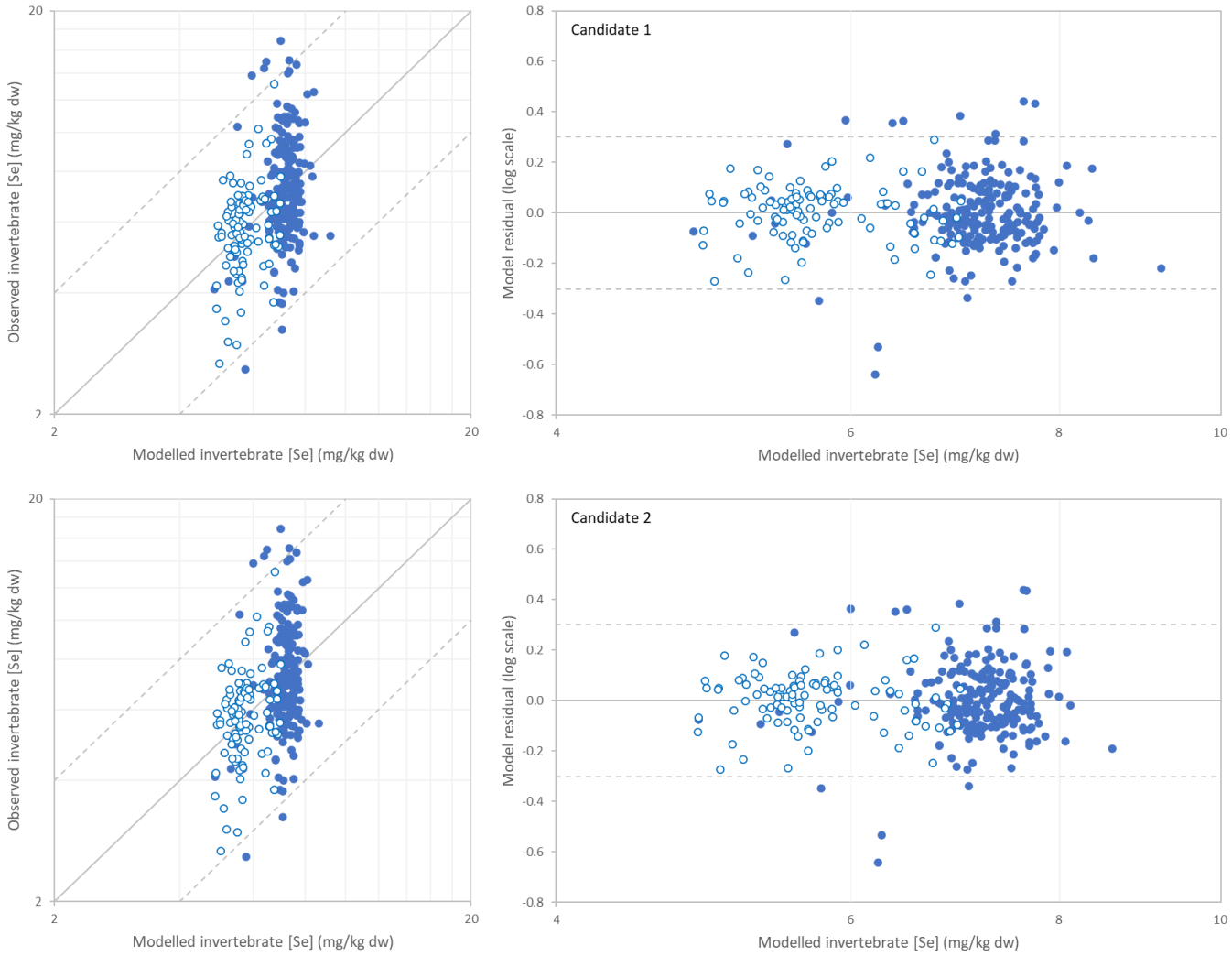

Figure 8. Model performance (left panels) and residuals (right panels) for candidate model coefficients fit to the full inorganic dataset (open symbols = selenite <0.05 µg/L; filled symbols = selenite ≥0.05 µg/L; candidate coefficient numbers as in Table 3)

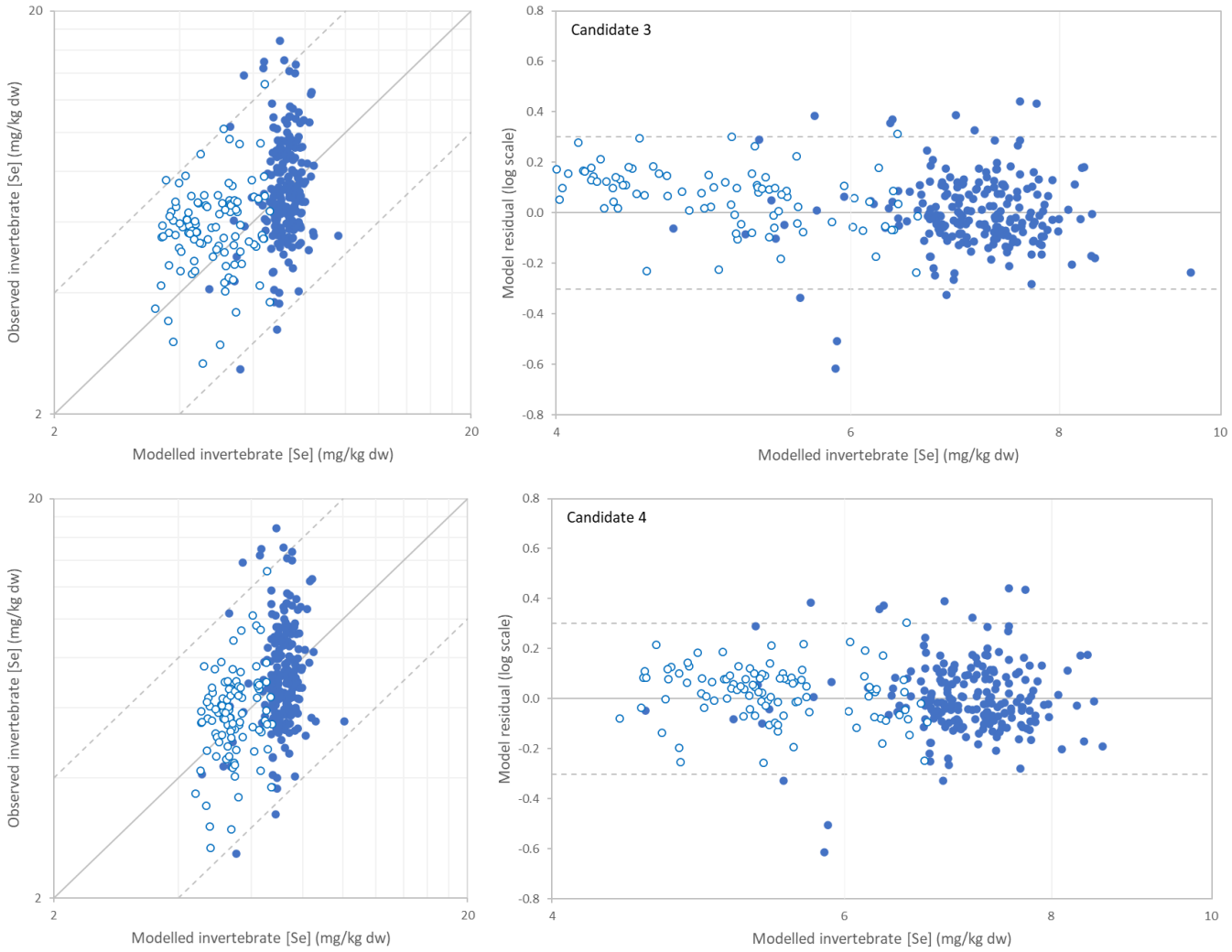

Figure 9. Model performance (left panels) and residuals (right panels) for candidate model coefficients fit to the constrained inorganic ([Se(IV)] >0.05 µg/L) dataset (open symbols = selenite <0.05 µg/L; filled symbols = selenite ≥0.05 µg/L; candidate coefficient numbers as in Table 3)

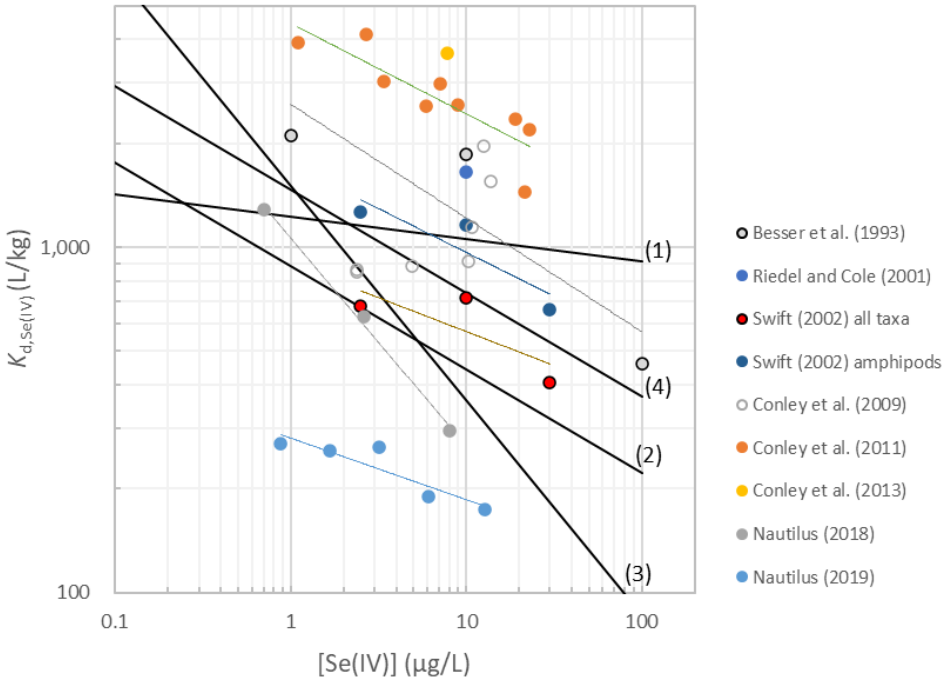

Figure 10. Candidate equations for selenite (black lines; candidate coefficient numbers as in Table 3) compared to laboratory data compiled by de Bruyn and Luoma (2021)

Recalibration of the Speciation Model: Organic Species

Recalibration of the organic species coefficients was conducted as follows:

- The analysis was conducting using the updated dataset described in the **Data Preparation** subsection above, filtered to retain only cases with detectable concentrations of one or more organic species (*n*=261)
- The same model form used in de Bruyn and Luoma (2021) was adopted, rearranged to give Equation 2
- Coefficients for selenate and selenite were fixed to the candidate 4 model discussed above
- The nonlinear regression function of Systat v13 was used to fit the coefficients in Equation 2 for DMSeO (a_{DMSeO}) and MeSe(IV) (a_{MeSeIV})
- To reduce effects of collinearity between DMSeO and MeSe(IV) and the influence of uncertainty in values less than the detection limit, the nonlinear regression was repeated using a constrained organoselenium dataset (*n*=83) that only included cases with detected concentrations (>0.01 µg/L) of both species
- After fitting a_{DMSeO} and a_{MeSeIV}, the dataset was filtered to include only cases with detectable MeSe(VI) (*n*=21) and the regressions were re-run (with a_{DMSeO} and a_{MeSeIV} fixed to the fitted values) to estimate a_{MeSeVI}; a similar analysis was conducted for a_{DMSe} (*n*=26) and a_{DMDSe} (*n*=4) but could detect no effect of either species
- Candidate fitted model coefficients were evaluated by inspecting regression statistics and model residuals when applied to the full dataset of all cases, both with and without detectable organoselenium
- To explore the robustness of fitted parameters, sensitivity analyses were conducted by fixing two of the coefficients, varying the remaining parameter across a wide range, and evaluating the resulting goodness of fit of the model to the full organic dataset

The fitted model form was:

$$log_{10}([Se]_{BI}) = log_{10}\begin{pmatrix}[SeVI] \times a_{SeVI} \times [SeVI]^{b_{SeVI}} \times [SO_4]^{b_{SO4}} + [SeIV] \times a_{SeIV} \times [SeIV]^{b_{SeIV}} \\ +[DMSeO] \times a_{DMSeO} + [MeSe(IV)] \times a_{MeSeIV} + [MeSe(VI)] \times a_{MeSeVI}\end{pmatrix} \quad \text{Equation 2}$$

where parameters and considerations are as in Equation 1.

Figure 5 shows the degree of collinearity between DMSeO and MeSe(IV) in the dataset used for this analysis. Points plotted off both the X- and Y-axes comprise the constrained subset of data (both species >0.01 µg/L) used to derive candidate 6. Fitted coefficients and regression statistics are provided in Table 4. Model fit and residuals are shown in Figure 11.

Table 4. Candidate model coefficients for organic species

Parameter	Candidate 5	Candidate 6
Adopted model for inorganic species	Candidate 4	Candidate 4
Data included	MeSe(IV) and/or DMSeO >0.01 µg/L; *n*=261	MeSe(IV) and DMSeO >0.01 µg/L; *n*=83
Mean Corrected r^2	0.595	0.446
a_{MeSeIV}	151 (126; 176); K_d=53,906	124 (68.0; 181); K_d=44,434
a_{DMSeO}	0 (-34.7; 34.7); K_d=0	10.3 (-51.6; 72.2); K_d=3,669
a_{MeSeVI}	0 (-47.6; 47.6); K_d=0	6.27 (-40.5; 53.1); K_d=2,238

Notes: See text for definitions of parameter names; values in parentheses are 95% confidence intervals on parameter estimates.

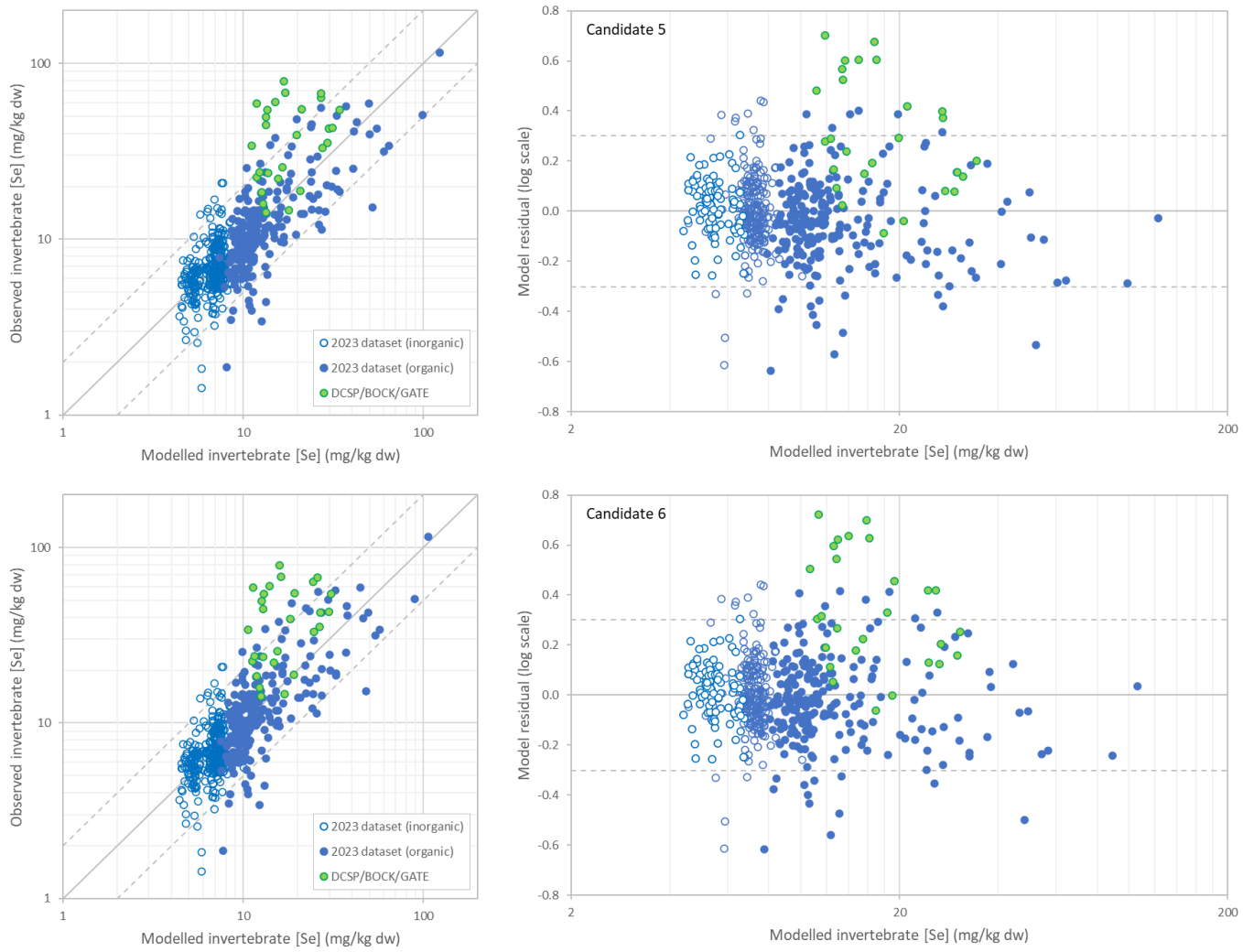

Figure 11. Model performance (left panels) and residuals (right panels) for candidate model coefficients applied to the full organic dataset (candidate coefficient numbers as in Table 4)

Both sets of candidate model coefficients provided similarly reasonable fit to the organic dataset (left panels of Figure 11) and both had acceptable residuals (right panels of Figure 11), with the exception of a cluster of relatively large positive residuals (>0.5 log units; underpredicted by more than a factor of 3) at modelled invertebrate selenium concentrations between 10 and 20 mg/kg dw. Inspection of these cases revealed that all were from sampling immediately downstream of the sedimentation ponds on EVO Dry Creek, Bodie Creek, and Gate Creek. Data from these sampling locations are plotted as green symbols on Figure 11, illustrating a consistent tendency to positive residuals that may relate to the relatively depositional habitat, silty substrate, and prevalence of infaunal taxa like chironomids in these three areas.

Both sets of candidate model coefficients gave a higher K_d for MeSe(IV) and a lower K_d for DMSeO than was estimated by de Bruyn and Luoma (2021). Candidate 5 assigned the entire effect of organoselenium on bioaccumulation to MeSe(IV), with an estimated K_d of 53,906, which is nearly double the estimate of 28,000 derived by de Bruyn and Luoma (2021). The inability of the candidate 5 analysis to detect an effect of the other

two organoselenium species may be a consequence of collinearity in the dataset. Candidate 6, which was derived from a constrained dataset that attempted to reduce collinearity, gave a slightly lower K_d for MeSe(IV) and was able to estimate K_d's for DMSeO and MeSe(VI). The estimated K_d for DMSeO in candidate 6 was 3,669, which is almost eight-fold lower than the value of 28,000 estimated by de Bruyn and Luoma (2021). The estimated K_d for MeSe(VI) in candidate 6 was 2,238, which is similar to the value of 2,000 estimated by de Bruyn and Luoma (2021).

Sensitivity of model fit to alternative coefficients is shown in Figure 12, expressed as the model sum of squared errors (SSE) calculated while varying one organic species coefficient (the one indicated by the label for each line) while holding the other two organic species coefficients constant at the fitted candidate values (indicated by the title of each plot). For comparison, the fit of the de Bruyn and Luoma (2021) coefficients to the full organic dataset is also shown. The lowest point of each line approximates the best model fit. The steepness of each curve indicates how sensitive model fit is to varying that coefficient across the plotted range.

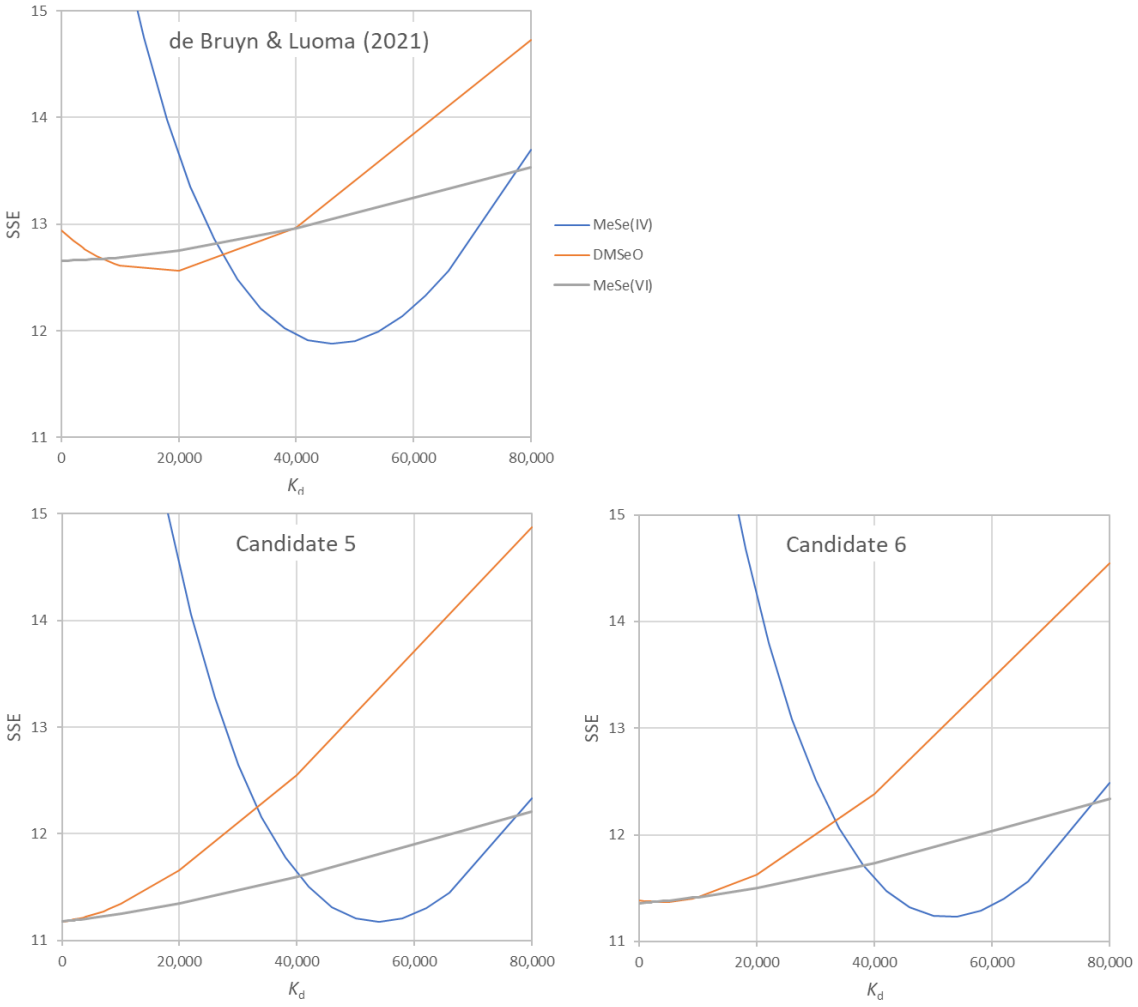

Figure 12. Sensitivity analysis for model coefficients applied to the full organic dataset (candidate coefficient numbers as in Table 4; see text for details)

Both candidate coefficient sets provided improved fit (lower SSE) compared to the de Bruyn and Luoma (2021) model (Figure 12). Results of the sensitivity analysis were as follows:

- Model fit was most sensitive to the coefficient for MeSe(IV), indicated by the steepness of the blue curves. There was little change in SSE between about 45,000 and 60,000 for all three coefficient sets evaluated on Figure 12. These patterns indicate that MeSe(IV) has a relatively large influence on model fit to this dataset, whether DMSeO is assigned a low K_d (zero in candidate 5) or a high K_d (28,000 in the de Bruyn and Luoma 2021 model). The steepness of the blue curves on Figure 12 suggests that the fitted coefficients for MeSe(IV) derived herein are relatively robust.
- Model fit was less sensitive to the coefficient for DMSeO, with little change in SSE between zero and about 10,000 for candidates 5 and 6. The SSE minimum occurred between about 10,000 and 20,000 for the de Bruyn and Luoma (2021) coefficient set because the K_d for MeSe(IV) was fixed at a lower value (28,000) than the optimal value for this dataset (~45,000) (but note that these minima give higher SSE than minima for the candidate 5 and 6 coefficient sets). These patterns indicate that DMSeO has a relatively small but likely non-zero influence on model fit to this dataset. The steepness of the orange curves on Figure 12 suggests that the fitted coefficients for DMSeO are not as robust as those for MeSe(IV), but that low values are best supported.
- Model fit was least sensitive to the coefficient for MeSe(VI), with little change in SSE between zero and about 20,000. SSE minima were near zero for all three coefficient sets evaluated on Figure 12. The influence of MeSe(VI) on bioaccumulation in this dataset is uncertain but likely low.

As discussed by de Bruyn and Luoma (2021), there are no other laboratory or field studies for comparison to K_d estimates for the organic species evaluated herein. Candidates 5 and 6 provided similar model performance (Figure 11). Candidate 6 was slightly better supported by the sensitivity analysis than candidate 5 (Figure 12) and was therefore selected as the preferred model.

Recalibration of the Speciation Model: Confidence and Prediction Intervals

Standard methods for defining confidence and prediction intervals for multiple regression models calculate the standard error of the prediction from the variance-covariance matrix of estimated regression coefficients. Unfortunately, the multi-step process used herein to overcome the problem of collinearity makes obtaining this matrix a non-trivial problem. In addition, calculating confidence and prediction intervals using these methods requires matrix algebra for every new prediction, which adds cumbersome elements to model application. Therefore, the following calculations used a practical alternative approach to approximate confidence and prediction intervals from the magnitude of residual variance around the fitted model. In essence, the modelled benthic invertebrate selenium concentration was treated as the predictor, and the standard error of the prediction could then be calculated using standard methods for a single-predictor regression.

The confidence interval on the mean model prediction was calculated as:

$$\hat{y}_h \pm t_{(1-\frac{\alpha}{2},n-2)} \times \sqrt{MSE \times \left(\frac{1}{n} + \frac{(x_h-\bar{x})^2}{\Sigma_i(x_i-\bar{x})^2}\right)} \qquad \text{Equation 3}$$

where $\hat{y}_h$ is the predicted value when the predictor is x_h. Both predictor and predicted value are $\log_{10}$ benthic invertebrate selenium concentrations. MSE is the mean square error (0.0298), n is the sample size (572), and $\bar{x}$ is

the mean predictor in the training dataset (0.950). MSE was calculated as the sum of squared errors (predictions minus observations, including all cases in the updated dataset) divided by *n*-2 degrees of freedom.

The prediction interval for new observations was calculated as:

$$\hat{y}_h \pm t_{(1-\frac{\alpha}{2},n-2)} \times \sqrt{MSE \times \left(1 + \frac{1}{n} + \frac{(x_h-\bar{x})^2}{\Sigma_i(x_i-\bar{x})^2}\right)} \quad \text{Equation 4}$$

where all terms are as in Equation 3.

For convenience, confidence and prediction intervals were calculated across the range of modelled benthic invertebrate selenium concentrations in the updated dataset, and then approximated using linear regression (prediction intervals) or polynomial regression (confidence intervals). The resulting equations provide very close approximations (r^2 >0.999) of the results of Equations 3 and 4.

The 95% confidence interval on the mean model prediction can be approximated as:

$$log_{10}UCL_h = 0.00568 + 1.01 \times log_{10}\hat{y}_h - 0.00149 \times (log_{10}\hat{y}_h)^2 \quad \text{Equation 5a}$$

$$log_{10}LCL_h = -0.00568 + 0.990 \times log_{10}\hat{y}_h + 0.00149 \times (log_{10}\hat{y}_h)^2 \quad \text{Equation 5b}$$

where UCL_h is upper confidence limit and LCL_h is the lower confidence limit at the predicted value $\hat{y}_h$.

The prediction interval for new observations can be approximated as:

$$log_{10}UPL_h = log_{10}\hat{y}_h + 0.339 \quad \text{Equation 6a}$$

$$log_{10}LPL_h = log_{10}\hat{y}_h - 0.339 \quad \text{Equation 6b}$$

where UPL_h is upper prediction limit and LPL_h is the lower prediction limit at the predicted value $\hat{y}_h$.

Confidence and prediction intervals for the recalibrated speciation model are shown in Figure 13.

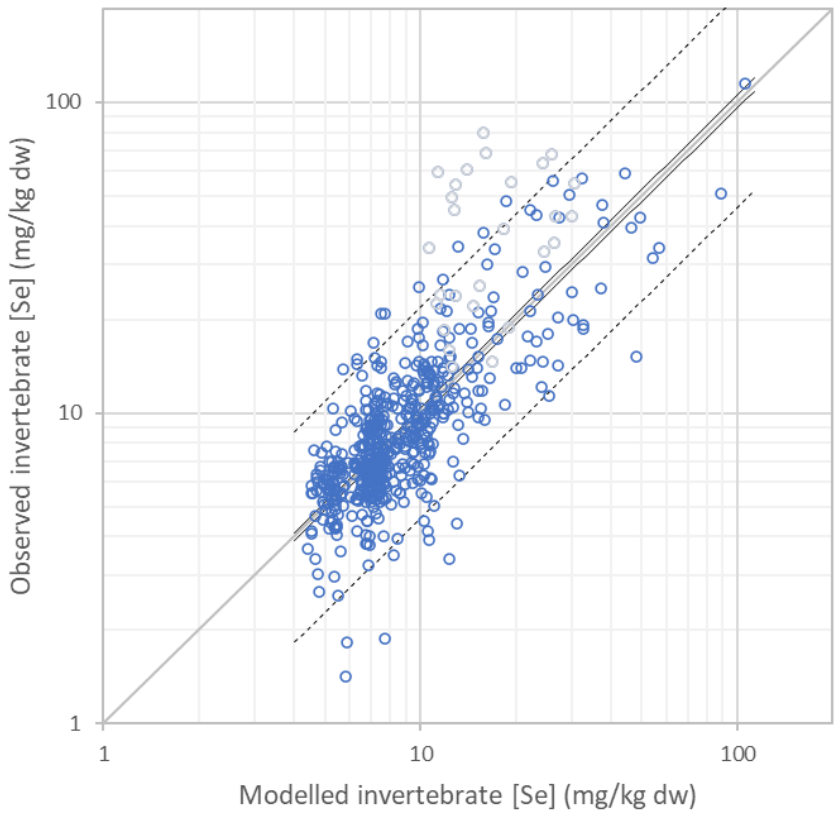

Figure 13. 95% confidence interval for the mean (solid black diagonals) and 95% prediction interval for new observations (dashed black diagonals) for the recalibrated speciation model (grey symbols are sampling locations in depositional habitats downstream of three sedimentation ponds; see text for details)

4.0 SUMMARY OF UPDATED MODELS

Current versions of all bioaccumulation model equations are summarized in Table 5. The following section outlines the recommended application of these model equations.

Table 5. Current versions of bioaccumulation model equations

Model	Equation
Total selenium, lotic	$[Se]_{BI} = 5.25 \times [Se]_{aq}^{0.071}$
Total selenium, lotic (with SO_4)	$[Se]_{BI} = 8.49 \times [Se]_{aq}^{0.143} \times [SO_4]^{-0.142}$
Total selenium, lentic	$[Se]_{BI} = 7.03 \times [Se]_{aq}^{0.397}$
Selenium speciation, lotic	$[Se]_{BI} = \begin{matrix}[SeVI] \times 7.94 \times [SeVI]^{-0.881} \times [SO_4]^{-0.126} + [SeIV] \times 4.13 \times [SeIV]^{-0.3} \\ +[MeSe(IV)] \times 124 + [DMSeO] \times 10.3 + [MeSe(VI)] \times 6.27\end{matrix}$

Notes: $[Se]_{BI}$ = benthic invertebrate selenium concentration (mg/kg dw); $[Se]_{aq}$ = aqueous total selenium concentration (µg/L); $[SO_4]$ = sulphate concentration (mg/L); [SeVI] = selenate concentration; [SeIV] = selenite concentration; [MeSe(IV)] = methylseleninic acid concentration; [DMSeO] = dimethylselenoxide concentration; [MeSe(VI)] = methaneselenonic acid concentration; all species concentrations in µg/L

As discussed in de Bruyn and Luoma (2021), each bioaccumulative selenium species is understood to contribute to total bioaccumulation additively and independently of other species. This interpretation is consistent with the current understanding that different selenium species are taken up by algae via different mechanisms, but that all are ultimately converted into the same suite of organic forms within the algal cell (Ponton et al. 2020).

Building on the concept of additivity across selenium species, the toolbox of model equations described in Sections 3.1 and 3.2 can be used in various combinations to model total bioaccumulation by adding together contributions from inorganic (selenate and selenite) and organic (DMSeO, MeSe(IV), and MeSe(VI)) species. Different combinations of model equations will provide the best tool for different situations, as outlined below.

Bioaccumulation of inorganic selenium in lotic areas should be modelled as follows:

- In lotic areas without material influence of organoselenium,[2] the lotic total selenium model (Section 3.1) would be the preferred approach because of the larger field dataset available to derive the model. The lotic total selenium model has been validated across a wide range of conditions throughout the Elk Valley and has been shown to give reliable predictions where there is no material contribution of organoselenium.
- Where there is a potential material influence of organoselenium, inorganic species should be modelled using the selenate and selenite terms of the speciation model (Section 3.2) where speciation data are available to support such modelling, or the lotic total selenium model (Section 3.1) where speciation data are not available.

Bioaccumulation of organoselenium in lotic areas should be modelled using the organoselenium terms of the speciation model (Section 3.2). These terms were derived from field studies in lotic areas exposed to a wide range of organoselenium concentrations in different combinations. The observation that bioaccumulation can be predicted from aqueous speciation in these areas supports the interpretation that direct uptake from the aqueous phase into algae is the dominant exposure pathway for lotic biota. The exception to this pattern occurs where there is a second exposure pathway. The clearest example of a second pathway is via accumulation and microbial processing of particulate-associated selenium in bryophyte mats in Erickson Creek. As discussed in Section 3.2, there may also be a second pathway in depositional lotic areas immediately downstream of the sedimentation ponds on EVO Dry Creek, Bodie Creek, and Gate Creek. To date, no other lotic area has been identified in the Elk Valley where there is a second exposure pathway that affects the reliability of predictions from the speciation model.

Bioaccumulation of selenium in lentic areas, including sedimentation ponds, should be modelled using the lentic total selenium model (Golder 2020). Lentic areas have multiple exposure pathways, with varying relative importance depending on the biogeochemical characteristics of the particular area. For example, lentic areas with organic sediment can have a material contribution of organoselenium from microbial processes in subsurface sediment (Martin et al. 2018). Aqueous speciation in overlying water may not capture all important exposure pathways at a fine enough spatial scale and therefore may not be a reliable predictor of bioaccumulation in lentic biota. There is not yet sufficient understanding of these pathways to model the relative importance of subsurface microbial processing, productivity of algae and microbes in soft sediment at the sediment-water interface,

[2] The current best criterion for evaluating organoselenium is the draft screening value of 0.025 µg/L, expressed as the sum of DMSeO and MeSe(IV). Concentrations greater than this value would indicate a potential material influence of organoselenium on bioaccumulation. Alternative criteria could be used, provided they support the same interpretation.

productivity of algae and microbes attached to plants, rocks, baffles, pond liners, or other surfaces above the sediment-water interface, and phytoplankton in the water column. Nor is there sufficient understanding of the characteristics and conditions of lentic areas that determine that relative importance and how it might vary seasonally or between years. At this time, the best available tool for modelling bioaccumulation is the lentic total selenium model. As discussed in Golder (2020), this model predicts bioaccumulation in "fully lentic" areas, which tend to have highly organic sediment and high vegetation cover. The model over-predicts bioaccumulation in areas with a lower degree of lentic character for the poorly-understood reasons discussed above.

Given the considerations outlined above, the recommended approach for different bioaccumulation modelling applications is as follows:

- In lotic areas with no expected material influence of organoselenium, the preferred tool for evaluating existing conditions is the lotic total selenium model.[3] Speciation data from these areas can be used to confirm the expectation that organoselenium is not contributing materially to bioaccumulation (or, alternatively, to indicate that another approach is warranted) and that proportions of selenate and selenite are consistent with the typical condition reflected in the lotic total selenium model. The lotic total selenium model is also the preferred tool for modelling expected future conditions from projected total selenium concentrations because these water quality model projections are well understood and routinely validated and recalibrated, whereas projections of speciation do not currently have the same level of reliability.
- In lotic areas with an expected material influence of organoselenium or with atypical proportions of selenate and selenite,[4] the preferred tool for evaluating existing conditions is the speciation model. Concentrations of all species can be obtained from the same analysis, which provides the best dataset for estimating the combined bioaccumulation from all detected species.
- In lotic areas with an expected material influence of organoselenium, the preferred tool for evaluating expected future conditions is to combine the lotic total selenium model (representing the best estimate of bioaccumulation of inorganic species from projected total selenium) with the organoselenium terms of the speciation model (representing the best estimate of the contribution of organoselenium species). Projected total selenium concentrations should be obtained from a reliable water quality model. Expected future organoselenium concentrations should be obtained using methods appropriate to the available information and future scenario being evaluated.
- The draft screening values for organoselenium should be revised to reflect the updated understanding of bioaccumulative potential of DMSeO and MeSe(IV) outlined in this memorandum.
- In lentic areas, the preferred tool for both existing and expected future conditions is the lentic total selenium model, noting that actual bioaccumulation will be lower than model predictions in areas that do not have all the characteristics of "fully lentic" areas.

[3] The lotic total selenium model equations with and without SO_4 give similar results under most conditions, and in most cases either could be used. If there is reason to suspect that the ratio of total selenium to SO_4 is inconsistent with the usual correlation of these two constituents in Elk Valley waters, the lotic total selenium model equation with SO_4 may provide a more accurate prediction.

[4] Selenite typically comprises ≤1% of total selenium and usually occurs at concentrations <1 µg/L in the Elk Valley.

5.0 CLOSURE

We trust that the information included in this technical memorandum meets your present requirements. Should you have any questions, please do not hesitate to contact the undersigned.

Adrian de Bruyn, PhD, RPBio
Owner, Senior Environmental Scientist

6.0 REFERENCES

ADEPT, Windward, and Minnow. 2023. Elk Valley Selenium Speciation Monitoring Program: 2022 Annual Report. Prepared for Teck Coal Limited. May 2023.

de Bruyn AMH, Luoma SN. 2021. Selenium Species Bioaccumulation Tool Draft Version 2.0. Prepared for Teck Coal Limited. February 2021.

Golder (Golder Associates Ltd). 2010. Selenium Bioaccumulation Analysis: Development of Site-Specific BAFs for Se in the Elk Valley. Prepared for Teck Coal Limited.

Golder. 2011. Line Creek Operations Phase II Project Environmental Assessment Certificate Application. Section B2.2. Aquatic Environment. Prepared for Teck Coal Limited. December 2011.

Golder. 2018a. Elk Valley Selenium Bioaccumulation Model Update. Prepared for Teck Coal Limited. January 2018.

Golder. 2018b. Selenium Species Bioaccumulation Tool Version 1.1. Prepared for Teck Coal Limited. May 2018.

Golder. 2020. Updates to the Lotic and Lentic Statistical Bioaccumulation Models for Selenium in the Elk Valley. Prepared for Teck Coal Limited. November 2020.

Martin AJ, Fraser C, Simpson S, Belzile N, Chen YW, London J, Wallschläger D. 2018. Hydrological and biogeochemical controls governing the speciation and accumulation of selenium in a wetland influenced by mine drainage. Environ. Toxicol. Chem. 37: 1824–1838.

Minnow Environmental Inc., Interior Reforestation Co. Ltd., and Paine, Ledge and Associates. 2011. Selenium Monitoring in the Elk River Watershed, B.C. (2009). Prepared for Teck Coal Limited. February 2011.

Orr PL, Wiramanaden CI, Paine MD, Franklin W, Fraser C. 2012. Food chain model based on field data to predict westslope cutthroat trout (*Oncorhynchus clarkii lewisi*) ovary selenium concentrations from water selenium concentrations in the Elk Valley, British Columbia. Environmental Toxicology and Chemistry 31: 672-680.

Ponton DE, Graves SD, Fortin C, Janz D, Amyot M, Schiavon M. 2020. Selenium interactions with algae: chemical processes at biological uptake sites, bioaccumulation, and intracellular metabolism. Plants 9: 528.

Teck. 2014. Elk Valley Water Quality Plan. Annex E: Baseline Derivation Report for Selenium.